Journal of Hydrology 546 (2017) 133–139

Contents lists available at ScienceDirect

Journal of Hydrology

journal homepage: www.elsevier.com/locate/jhydrol

Research papers

# Root channels to indicate the increase in soil matrix water infiltration capacity of arid reclaimed mine soils

Gao-Lin Wu [a,b,c,1], Yu Liu [a,c,1], Zheng Yang [a], Zeng Cui [a,b], Lei Deng [a,c], Xiao-Feng Chang [a,c], Zhi-Hua Shi [a,c,d,*]

[a] State Key Laboratory of Soil Erosion and Dryland Farming on the Loess Plateau, Northwest A & F University, Yangling, Shaanxi 712100, China
[b] State Key Laboratory of Grassland Agro-Ecosystems, College of Pastoral Agriculture Science and Technology, Lanzhou University, Lanzhou 730020, China
[c] Institute of Soil and Water Conservation, Chinese Academy of Sciences and Ministry of Water Resource, Yangling, Shaanxi 712100, China
[d] College of Resources and Environment, Huazhong Agricultural University, Wuhan 430070, China

ARTICLE INFO

*Article history:*
Received 3 November 2016
Received in revised form 12 December 2016
Accepted 23 December 2016
Available online 10 January 2017
This manuscript was handled by G. Syme, Editor-in-Chief

*Keywords:*
Soil infiltration rate
Root channels
Artificial grassland
Arid area

ABSTRACT

Soil matrix flow plays a critical role in redistributing the precipitation input and enhancing water storage in arid areas. Root channels can result in macropore flow which strongly influences soil infiltration. Prior research has addressed the influence of vegetation on erosion and runoff, but the effects of root channels on infiltration capacity are less studied. In this study, we studied the root channels and soil water infiltration rates in ten artificial grasslands in an arid area. The results showed that the average root channel diameter (ARCD) of leguminous grasslands and of shrub grasslands were greater than that of gramineous grasslands ($p < 0.05$). Importantly, the ARCD and root channel area (RCA) were significantly and positively related to the average infiltration rate in stage I (AIRS I) and the initial infiltration rate (IIR). The IIR and the AIRS I increased at rates of 31.13 and 14.60 mm $h^{-1}$, respectively, and at the same time there was an increase in ARCD. Overall, our results suggest that root channels played a significant role in the matrix infiltration capacity, resulting in a higher infiltration rate in leguminous grasslands and in mixed sown grasslands than in gramineous grasslands. We suggest that leguminous grasslands or the combination of leguminous and gramineous species in grassland should be given greater attention as suitable materials for mine-soil reclamation in arid regions. Our research improve the understanding of the influence of vegetation on soil hydrological processes and of the hydrology of reclaimed mine soils in arid regions.


## 1. Introduction

Surface mining for ores has a profound effects on landscapes and influences water resources in many world regions, making methods for restoring environmental quality on mine sites is a common research topic (Atanackovíc et al., 2013; Clark and Zipper, 2016; Younger and Wolkersdorfer, 2004). As a principle method to restore environmental quality, vegetation establishment is commonly viewed as a continuous process – from establishment of the new vegetation to the sustainable development – to improve ecosystem resilience and stability on mine sites in both the short- and long-term (Yang et al., 2012; Zhu et al., 2009). The establishment and development of grassland on mine sites contributes to the restoration of hydrological processes, including infiltration capacity and erosion control (Clark and Zipper, 2016; Moreno-de las Heras et al., 2009). Moreover, grassland has a dense root system that not only ensures survival of the ecosystem given multiple pressures (e.g., extreme climatic events and poor soil) but also helps to improve the surface soil properties (Shi et al., 2012; Wu et al., 2014). As a result, the role of grassland in controlling soil erosion has been paid a great deal of attention in arid and semi-arid zones (Wu et al., 2016a).

Coal surface mining typically displaces large amounts of earth materials. Following coal extraction, the displaced materials are placed on the mined surface as "mine spoil", which is often developed into a post-mining landform that includes vegetation (Clark and Zipper, 2016). In both arid and semi-arid areas, soil infiltration is recognized as a fundamental ecological process that affects the water budget of vegetation (Michaelides et al., 2009). Artificial grassland could ameliorate the soil infiltration capacity and influence soil water redistribution processes by root systems (Neris et al., 2012). Water shortage is a limiting factor that affects ecological recovery in arid areas (Khan et al., 2009). Thus, maximizing the soil retention of precipitation and reducing runoff are crucial for the ecological restoration in arid areas (Shi and Shao, 1999). The

* Corresponding author at: Institute of Soil and Water Conservation, Chinese Academy of Sciences and Ministry of Water Resources, 26 Xinong Road, Yangling, Shaanxi 712100, PR China.
*E-mail address:* shizhihua70@gmail.com (Z.-H. Shi).
[1] These authors contributed equally to this work.

http://dx.doi.org/10.1016/j.jhydrol.2016.12.047
0022-1694/

soil properties play a crucial role in the process of soil infiltration (Cerdà, 1997). Many studies about soil infiltration capacity have drawn attention to the effects of soil properties and changes in land use (Neris et al., 2012). Moreover, the effect of macropores on water flow in soils is an important soil science research topic (Beven and Germann, 2013; Xin et al., 2016). Macropore flow processes are often not considered in hydrological rainfall-runoff models, where soils are usually treated as a continuous porous medium and flow only depends on the hydraulic conductivity and the water content in the soil (Weiler and Naef, 2003). Root channels are voids biopores formed by plant roots. Water flow in root channels is an important mechanism of infiltration in soil and is crucial for the prediction of runoff generation and groundwater recharge (Weiler and Naef, 2003). Macropores formed by the root systems of vegetation are important conduits for downward water movement in grasslands. Root channels generate soil macroporosity resulting in higher infiltration than expected based solely on the textural properties of the surface soil (Van Schaik, 2009). The flow resulting from root channels may produce a lateral flow component and result in rapid percolation to groundwater and stream flow after a rainfall event. This process can affect erosion processes and the transport of solutes and pollution (Rechel and Carter, 1992; Van Schaik, 2009). Devitt and Smith (2002) also found that plant root systems in desert soils increase downward water flux to deeper soil depths via root channels, the effect of which becomes more pronounced with an increase in the size of the plant root system.

Various soil infiltration measurement methods have been developed, such as the double-ring method, the rainfall simulator, the disc permeameter, and the point source method (Mao et al., 2011, 2016). The double-ring method is unable to accurately measure infiltration rates in ecosystems with an insufficient water supply. The occurrence of water leakage with the disc permeameter during experiments could negatively affect the accuracy of measurements. The rainfall simulator does not function well under conditions of intense rainfall since it cannot accurately measure a high initial infiltration (Mao et al., 2011). Using the point source method, a circular or nearly circular wet area is formed at the soil surface, which increases gradually over time (Mao et al., 2016). Compared with the other methods, the point source method required little water and time, and had a high accuracy for determination of soil infiltration.

In this study, ten types of artificial grassland on a post-mining landform – all reclaimed with similar techniques – were studied. Our objective was to evaluate the effects of plant root channels on infiltration rates in different artificial grassland. The results from this study can inform reclamation scientists of techniques to increase infiltration capacity (i.e., infiltration rate) in reclaimed landscapes, including the use of different plant species compositions.

## 2. Materials and methods

### 2.1. Study sites

The present study was conducted on a post-mining landform of the Yongli coal mine, Inner Mongolian Autonomous Region, located in the northern Loess Plateau (110° 16′ 30″ E, 39° 41′ 52″N, H: 1026–1304 m) of China. The area is characterized by a semiarid climate, with a mean annual temperature of 7.2 °C and an average annual precipitation of 404.1 mm, 80% of which falls from July to September. The annual evaporation is 2082.2 mm and the annual cloud-free solar radiation is approximately 3119.3 h. The climate is cold and dry in the winter and spring, and rainy and hot in the summer. The main soil is sandy soil (Calcaric Cambisols, FAO) and the soil thickness is approximately 50 cm. The mean soil fraction contents are sand, 53%; silt, 42%; and clay, 5% (determined by laser diffraction using a Mastersizer 2000, Malvern Instruments). The main plant species in the region are *Artemisia sacrorum*, *Stipa capillata*, *Artemisia desterorum*, and *Lespedeza bicolor*.

### 2.2. Experiment design

Ten artificial grassland types were established for study on flat reclaimed land in June 2012 (Fig. 1): five leguminous grasslands each with a different monoculture of *Medicago sativa* (Ms), *Astragalus adsurgens* (Aa), *Lespedeza davurica* (Ld), *Hedysarum scoparium* (Hs), or *Hedysarum mongolicum* (Hm); two gramineous grasslands each with a different monoculture of *Agropyro mongolicum* (Am), or *Bromus inermis* (Bi); and three mixed sown grasslands each with a different two-species intercrop of *Agropyron mongolicum* + *Artemisia desertorum* (Am + Ad), *Astragalus adsurgens* + *Artemisia desertorum* (Aa + Ad), or *Medicago sativa* + *Bromus inermis* (Ms + Bi). Among the plant species, Hm, Hs and Ad are shrubs whereas the others are herbs. Ms and Bi are the most common species used in vegetation restoration in China and can improve soil properties rapidly. Aa, Am, Ld and Hs are dominant species of this region and survive easily in arid environments. Ad is a pioneer species in community succession and an indicator of specific soil properties. Six replicate plots (3.0 m × 5.0 m) arranged within two blocks were established for each grassland type (Fig. 1). All treatments had the same soil conditions as determined before establishing the blocks. Seeds were planted with a row spacing of 50 cm and a sowing rate of 0.07 kg $m^{-2}$. Since the soil was barren, the sowing rate was increased slightly to guarantee a high emergence rate allowing for a rapid growth of dense plant populations with widespread cover. To ensure survival at the beginning of restoration, the grass species were established at the same plant density and irrigated with same amounts of water. Thereafter, grass growth mainly depended on rainfall; there was no additional fertilization or animal disturbance. We strived for similar conditions in all plots, to be able to attribute differences in soil infiltration solely to the type of artificial grassland. No plants were harvested during the experiment to guarantee a natural succession.

### 2.3. Soil sampling and laboratory analysis

At the peak of the growing season (September), we randomly selected two parallel 1.0 m × 1.0 m quadrats in each plot for further study. Above-ground biomass (AGB) was harvested at soil level and placed into an envelope. Each envelope was weighed fresh and then re-weighed after drying at 65 °C for 48 h. The thickness of the mine soil is about approximately 50 cm and the plant roots are mainly distributed in the 0–30 cm soil layer in the study area (Wu et al., 2016c). Therefore, to measure the below-ground root biomass, a 9 cm diameter root auger was used to collect three soil samples for each depth level of 0–10 cm, 10–20 cm, 20–30 cm; the samples were mixed for each depth level to create a single sample per depth level. A 2 mm sieve was used to isolate the majority of plant roots from each sample, and the isolated roots were oven-dried at 75 °C and then weighed.

The soil bulk density (BD; g $cm^{-3}$) of the different soil layers was measured using a soil bulk sampler with a 5 cm diameter and 5 cm high stainless steel cutting ring at points adjacent to the soil sampling quadrants. There were five replicates for each soil layer. The original volume of each soil core and its dry mass after oven-drying at 105 °C were measured. The gravimetric soil water content (SWC, %) was determined for each sample by taking the proportion of the loss of mass during oven drying at 105 °C to the constant mass. The soil organic matter content (SOM, g $kg^{-1}$) was measured by the vitriol acid-potassium dichromate oxidation

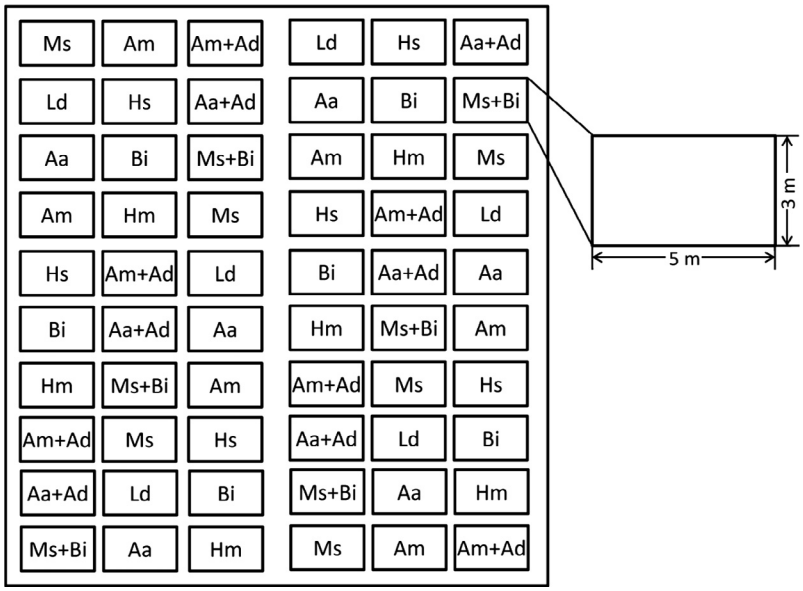


**Fig. 1.** Experimental design of treatments as arranged in plots and blocks. Note: *Medicago sativa*, Ms; *Lespedeza davurica*, Ld; *Astragalus adsurgens*, Aa; *Agropyron mongolicum*, Am; *Bromus inermis*, Bi; *Hedysarum scoparium*, Hs; *Hedysarum mongolicum*, Hm; *Agropyron mongolicum* + *Artemisia desertorum*, Am + Ad; *Astragalus adsurgens* + *Artemisia desertorum*, Aa + Ad; *Medicago sativa* + *Bromus inermis*, Ms + Bi.

method (Wu et al., 2016b). The soil total porosity (TP, %) was calculated using the formula (1-BD/PD) × 100, where BD is the bulk density (g cm$^{-3}$) and PD is the particle density (g cm$^{-3}$) which was assumed to be 2.65 g cm$^{-3}$ (Wang and Shao, 2013).

### 2.4. Root channels measurement

The below-ground biomass was harvested at each soil level in each quadrat, and a Vernier caliper was used to measure the diameter of the root channels (the diameter of stubble on the ground) in 1/4 quadrats (each quadrat was evenly divided into four parts); and measurements from the 1/4 quadrats were averaged to determine the average root channels diameter (ARCD) per quadrat. The total number of root channels in each quadrant was calculated and used to estimate the root channel area (RCA) per quadrat. The formulas used were the following:

$$\mathrm{ARCD} = \sum_{i=1}^{n} d_i/n \ (n = 1, 2, 3\ldots) \quad (1)$$

$$\mathrm{RCA} = N\pi\mathrm{ARCD}^2/4S \ (N = 1, 2, 3\ldots) \quad (2)$$

where $d$ is the diameter of the root channel (mm); $n$ is the number of root channels in 1/4 of the quadrat (2500 cm$^2$); $N$ is the number of root channels in the quadrat; and $S$ is the area of the quadrat (1 m$^2$ = 10,000 cm$^2$).

### 2.5. Soil infiltration rate measurement

The soil infiltration rates for the different artificial grasslands were determined using the soil infiltration capacity automatic measurement system (Mao et al., 2011; Lei et al., 2013). This system comprises a camera, a computer, a peristaltic pump and a tripod. The camera automatically captures images of the wet area every 3 min while the peristaltic pump is working. We used a numerical algorithm to calculate the capacity of soil infiltration (Lei et al., 2007, 2010, 2013). The model incorporation the numerical algorithm could calculate the infiltration rate at different times (Lei et al., 2010, 2013). The formula used to determine the soil infiltration rate is the following:

$$i_n = \frac{q - \sum_{j=1}^{n-1} i_j \Delta A_{n-j+1}}{\Delta A_n} \quad (n = 1, 2, 3\ldots) \quad (3)$$

where $q$ is the water flow rate (in this experiment, the water flow rate is 3.0 L h$^{-1}$); $i_n$ is the soil infiltration rate at time $t_n$, (mm h$^{-1}$); and $\Delta A_n$ is the increase of wet area for a given time period ($t_n - t_{n-1}$) (mm$^2$) (Wu et al., 2016c).

According to the methods of Wu et al. (2016c), we divided the process of soil infiltration into four stages: the initial average infiltration rate for the first 3 min (IIR), the average infiltration rate of stage I for 0–15 min (AIRS I), the average infiltration rate of stage II for 15–45 min (AIRS II), the average infiltration rage of stage III for 45–75 min (AIRS III), the average steady infiltration rate for the final 3 min (SIR), and the overall average infiltration rate for the 0–75 min period (AIR) (Fig. 2).

### 2.6. Statistical analysis

Linear mixed-effect modeling was used to analyze the ARCD, RCA and soil properties in the ten different grasslands. The species composition of each plot was considered as fixed effect in the analyses, and block and plot (nested within block) were considered as random effects. We used the function 'lme' in the package 'nlme' (Pinheiro et al., 2016) for linear mixed-effects modeling in R statistical software (version 3.3.1; R Development Core Team 2016). Regression analysis was used to determine relationships between the diameter of root channels, the area of root channels and the infiltration rate at different stages (e.g., IIR, AIRS, AIR). Tukey's post hoc test was used to carry out the multiple comparisons. Significant differences were evaluated at the 0.05 probability level and all data were expressed as the mean values ± standard error (M ± S.E.).

## 3. Results

### 3.1. Soil properties in different grasslands

The differences in the soil physical properties of the different grassland types are shown in Table 1. The Am + Ad grassland had

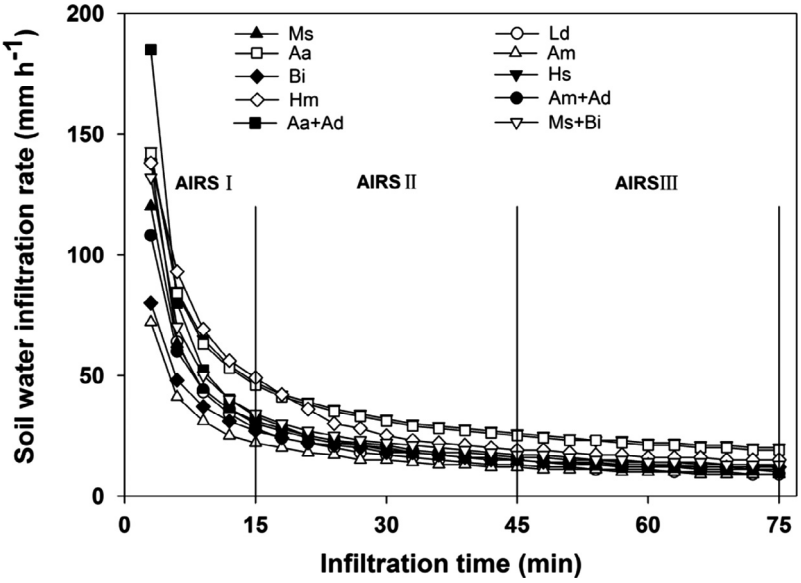


**Fig. 2.** The soil water infiltration rates with time under different artificial grassland types. Note: *Medicago sativa*, Ms; *Lespedeza davurica*, Ld; *Astragalus adsurgens*, Aa; *Agropyron mongolicum*, Am; *Bromus inermis*, Bi; *Hedysarum scoparium*, Hs; *Hedysarum mongolicum*, Hm; *Agropyron mongolicum* + *Artemisia desertorum*, Am + Ad; *Astragalus adsurgens* + *Artemisia desertorum*, Aa + Ad; *Medicago sativa* + *Bromus inermis*, Ms + Bi.

**Table 1**
Soil properties in different artificial grasslands.

| Grassland types | SOM (g kg$^{-1}$) | pH | BGB (g m$^{-2}$) | SWC (%) | BD (g cm$^{-3}$) | TP (%) |
|---|---|---|---|---|---|---|
| Ms | 6.78 ± 0.97bcd | 8.04 ± 0.04a | 627.06 ± 123.96ab | 10.25 ± 0.21ab | 1.52 ± 0.01bc | 42.77 ± 0.02bc |
| Ld | 8.00 ± 1.01ab | 8.04 ± 0.07a | 134.51 ± 26.82b | 12.69 ± 0.57a | 1.49 ± 0.01bc | 43.68 ± 0.53ab |
| Aa | 5.10 ± 0.15 cd | 8.04 ± 0.04a | 412.86 ± 93.62ab | 9.97 ± 0.36ab | 1.46 ± 0.01bc | 44.82 ± 0.21a |
| Am | 6.36 ± 0.61bcd | 8.00 ± 0.07a | 573.33 ± 122.01ab | 12.11 ± 0.54ab | 1.50 ± 0.01bc | 43.41 ± 0.39ab |
| Bi | 6.73 ± 0.18bcd | 7.97 ± 0.07a | 762.35 ± 195.82a | 12.46 ± 0.71a | 1.56 ± 0.01ab | 41.00 ± 0.12 cd |
| Hs | 4.35 ± 0.34d | 8.17 ± 0.11a | 739.02 ± 10.39a | 8.97 ± 2.06b | 1.47 ± 0.02bc | 44.65 ± 0.73ab |
| Hm | 7.48 ± 0.49abc | 8.15 ± 0.07a | 542.98 ± 65.49ab | 11.16 ± 0.69ab | 1.61 ± 0.01a | 39.28 ± 0.06d |
| Am + Ad | 5.87 ± 0.18bcd | 8.09 ± 0.08a | 436.94 ± 133.75ab | 10.85 ± 0.52ab | 1.39 ± 0.01d | 47.62 ± 0.07a |
| Aa + Ad | 9.42 ± 0.16a | 8.06 ± 0.07a | 342.68 ± 23.54ab | 10.23 ± 0.36ab | 1.47 ± 0.01bc | 44.52 ± 0.54ab |
| Ms + Bi | 8.17 ± 0.08ab | 7.97 ± 0.11a | 560.33 ± 139.87ab | 11.30 ± 0.94ab | 1.45 ± 0.01c | 45.24 ± 0.32a |

Note: *Medicago sativa*, Ms; *Lespedeza davurica*, Ld; *Astragalus adsurgens*, Aa; *Agropyron mongolicum*, Am; *Bromus inermis*, Bi; *Hedysarum scoparium*, Hs; *Hedysarum mongolicum*, Hm; *Agropyron mongolicum* + *Artemisia desertorum*, Am + Ad; *Astragalus adsurgens* + *Artemisia desertorum*, Aa + Ad; *Medicago sativa* + *Bromus inermis*, Ms + Bi. SOM, soil organic matter; BGB, below-ground biomass; SWC, soil water content; BD, soil bulk density; TP, soil total porosity. The lower-case letters indicate significant differences at the $p < 0.05$ probability level.

a significantly lower BD but a higher TP than the other grasslands ($p < 0.05$). Soil organic matter in the Aa + Ad grassland (9.42 ± 0.16 g kg$^{-1}$) was significantly higher than in the Hs grassland (4.35 ± 0.34 g kg$^{-1}$). Species composition had a significant effect on SOM (Table 2). There was no significant difference in pH among the grassland types ($p > 0.05$). The below-ground biomass in the Hs grassland (739.02 ± 10.39 g m$^{-2}$) and in the Bi grassland (762.35 ± 195.82 g m$^{-2}$) was significantly higher than in the Ld grassland (134.51 ± 26.82 g m$^{-2}$) ($p < 0.05$). However, SWC in the Ld grassland (12.69 ± 0.57%) and in the Bi grassland (12.46 ± 0.71%) was significantly higher than in the Hs grassland (8.97 ± 2.06%) ($p < 0.05$). The F-values and *p*-values calculated from the linear mixed models for the soil properties in the different grasslands are presented in Table 2.

**Table 2**
F-values and p-values of statistical tests comparing the soil properties and root channel characteristics among artificial grassland types.

| Response variable | Species | |
|---|---|---|
| | F-value | *p*-value |
| Soil organic matter (g kg$^{-1}$) | **4.59** | **0.04** |
| Soil pH | 0.66 | 0.42 |
| Below-ground biomass (g m$^{-2}$) | 0.72 | 0.40 |
| Soil water content (%) | 0.02 | 0.96 |
| Soil bulk density (g cm$^{-3}$) | 3.16 | 0.08 |
| Soil total porosity (%) | 3.59 | 0.07 |
| Diameter of root channels (mm) | 0.45 | 0.51 |
| Area of root channels (mm$^2$ cm$^{-2}$) | 0.84 | 0.36 |

Note: F-values and *p*-values were calculated from linear mixed-effects models. Bold values indicate significant differences at the $p < 0.05$ probability level.

### 3.2. Root channels of different artificial grasslands

The average root channels diameters were significantly different among the artificial grasslands ($F = 6.413$, $p < 0.01$) (Fig. 3a). The ARCD of the Am grassland (0.82 ± 0.17 mm) and Am + Ad grassland (1.08 ± 0.21 mm) were lower than those of the Aa grassland (2.26 ± 0.35 mm), Hs grassland (2.42 ± 0.50 mm) and Aa + Ad grassland (2.62 ± 0.27 mm) grasslands. There was a significant difference in the RCA among the different artificial grasslands ($F = 2.59$, $p = 0.02$) (Fig. 3b). The RCA of the Am grassland (0.21 ± 0.06 mm$^2$ cm$^{-2}$) was the lowest among the grasslands. The RCA of the Aa + Ad grassland (1.12 ± 0.30 mm$^2$ cm$^{-2}$) was the highest among the grasslands and was 49.3% higher than that of the Aa grassland (0.75 ± 0.20 mm$^2$ cm$^{-2}$).

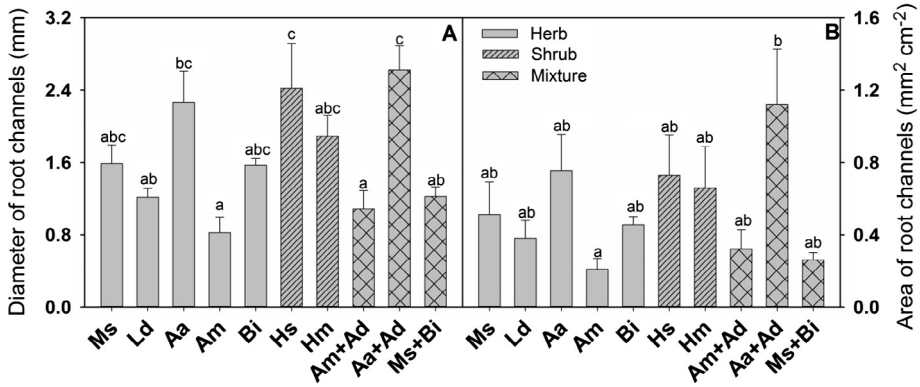


**Fig. 3.** The average diameter (A) and area of root channels (B) under different artificial grasslands. Note: *Medicago sativa*, Ms; *Lespedeza davurica*, Ld; *Astragalus adsurgens*, Aa; *Agropyron mongolicum*, Am; *Bromus inermis*, Bi; *Hedysarum scoparium*, Hs; *Hedysarum mongolicum*, Hm; *Agropyron mongolicum* + *Artemisia desertorum*, Am + Ad; *Astragalus adsurgens* + *Artemisia desertorum*, Aa + Ad; *Medicago sativa* + *Bromus inermis*, Ms + Bi.

### 3.3. Soil water infiltration in different artificial grasslands

The soil water infiltration process of the different artificial grasslands can be divided into three stages (Table 3). The AIR, AIRS II, AIRS III and SIR of the leguminous grasslands were higher than those of the gramineous grasslands. The IIRs of the Am grassland and the Bi grassland were the lowest among the grasslands; the AIRS I and the IIR of the Hs grassland and the Hm grassland were significantly higher than the other artificial grasslands. The IIR of the Am + Ad grassland increased by 22.7% when compared with the Am grassland, while the IIR of the Aa + Ad grassland and the Aa grassland were basically identical. For SIR, we found the opposite trend: the SIR of the Am + Ad grassland and the Am grassland were basically identical, whereas the SIR of the Aa + Ad grassland was lower than that of the Aa grassland by 33.1%. The IIR of the Ms + Bi grassland was lower than that of the Ms grassland by 29.4% and higher than that of the Bi grassland by 45.9%.

Correlation analyses showed that for the different artificial grasslands the ARCD and RCA were significantly and positively related to the AIR and to the AIRS, while there was no significant relationships with AIRS II (except for ARCD in leguminous grassland), AIRS III, or SIR (Table 4).

**Table 3**
Water infiltration rate (M ± S.E.) in different artificial grasslands.

| Grassland types | AIR (mm h$^{-1}$) | AIRS I (mm h$^{-1}$) | AIRS II (mm h$^{-1}$) | AIRS III (mm h$^{-1}$) | IIR (mm h$^{-1}$) | SIR (mm h$^{-1}$) |
|---|---|---|---|---|---|---|
| Ms | 27.49 ± 1.49 | 75.08 ± 10.87 | 20.98 ± 1.87 | 13.33 ± 1.86 | 142.67 ± 33.17 | 12.67 ± 1.86 |
| Ld | 26.81 ± 6.11 | 72.08 ± 14.83 | 20.79 ± 5.15 | 13.00 ± 3.36 | 132.67 ± 26.46 | 12.33 ± 3.17 |
| Aa | 33.75 ± 5.87 | 83.00 ± 9.75 | 27.64 ± 5.73 | 17.81 ± 3.99 | 139.00 ± 6.81 | 16.78 ± 3.78 |
| Am | 28.19 ± 6.97 | 57.67 ± 10.81 | 24.95 ± 6.71 | 17.81 ± 5.33 | 88.00 ± 12.66 | 17.11 ± 5.15 |
| Bi | 22.67 ± 0.95 | 45.67 ± 2.20 | 20.17 ± 1.20 | 14.52 ± 1.16 | 69.00 ± 5.86 | 14.00 ± 1.15 |
| Hs | 34.61 ± 8.26 | 91.50 ± 20.41 | 27.05 ± 6.98 | 17.24 ± 4.71 | 167.33 ± 36.44 | 16.33 ± 4.51 |
| Hm | 27.93 ± 2.78 | 77.92 ± 7.17 | 21.21 ± 2.58 | 12.81 ± 1.49 | 139.33 ± 13.30 | 12.11 ± 1.49 |
| Am + Ad | 30.03 ± 2.61 | 66.83 ± 3.55 | 25.67 ± 2.72 | 17.71 ± 2.22 | 108.00 ± 5.19 | 16.89 ± 2.12 |
| Aa + Ad | 25.97 ± 1.19 | 73.75 ± 8.17 | 19.36 ± 0.23 | 11.90 ± 0.42 | 142.33 ± 22.62 | 11.22 ± 0.40 |
| Ms + Bi | 25.27 ± 3.64 | 59.58 ± 7.72 | 21.02 ± 3.59 | 14.14 ± 2.94 | 100.67 ± 15.76 | 13.56 ± 2.80 |

Note: *Medicago sativa*, Ms; *Lespedeza davurica*, Ld; *Astragalus adsurgens*, Aa; *Agropyron mongolicum*, Am; *Bromus inermis*, Bi; *Hedysarum scoparium*, Hs; *Hedysarum mongolicum*, Hm; *Agropyron mongolicum* + *Artemisia desertorum*, Am + Ad; *Astragalus adsurgens* + *Artemisia desertorum*, Aa + Ad; *Medicago sativa* + *Bromus inermis*, Ms + Bi; AIR, the average infiltration rate; AIRS I, AIRS II and AIRS III, the average infiltration rate in stage I, II and III, respectively; IIR, the initial infiltration rate; SIR, the steady infiltration rate.

**Table 4**
The correlation matrix (Pearson correlation coefficient) of infiltration rates, diameter of root channels and area of root channels among different types of artificial grasslands.

| | AIR (mm h$^{-1}$) | AIRS I (mm h$^{-1}$) | AIRS II (mm h$^{-1}$) | AIRS III (mm h$^{-1}$) | IIR (mm h$^{-1}$) | SIR (mm h$^{-1}$) |
|---|---|---|---|---|---|---|
| ARCD-L (mm) | 0.56$^{*}$ | 0.56$^{*}$ | 0.47$^{*}$ | 0.36 | 0.47$^{*}$ | 0.33 |
| RCA-L (mm$^2$ cm$^{-2}$) | 0.56$^{*}$ | 0.70$^{**}$ | 0.38 | 0.21 | 0.68$^{**}$ | 0.17 |
| ARCD-G (mm) | 0.51 | 0.89$^{**}$ | 0.40 | 0.28 | 0.92$^{**}$ | 0.27 |
| RCA-G (mm$^2$ cm$^{-2}$) | 0.54 | 0.94$^{**}$ | 0.43 | 0.31 | 0.97$^{**}$ | 0.29 |
| ARCD-M (mm) | 0.29 | 0.63$^{*}$ | 0.20 | 0.13 | 0.64$^{*}$ | 0.14 |
| RCA-M (mm$^2$ cm$^{-2}$) | 0.55 | 0.74$^{*}$ | 0.45 | 0.38 | 0.68$^{*}$ | 0.38 |
| ARCD-T (mm) | 0.33$^{*}$ | 0.58$^{**}$ | 0.21 | 0.10 | 0.60$^{**}$ | 0.08 |
| RCA-T(mm$^2$ cm$^{-2}$) | 0.30 | 0.61$^{**}$ | 0.14 | 0.02 | 0.67$^{**}$ | 0.01 |

Note: AIR, the average infiltration rate; AIRS I, AIRS II and AIRS III, The average infiltration rate in stage I, II and III; IIR, the initial infiltration rate; SIR, the steady infiltration rate; ARCD, the average root channel diameter; RCA, the root channel area; L, G, M, T, legume grasslands, gramineous grasslands, mixed sown grasslands, and all grasslands types respectively.

$^{*}$ Correlation is significant at the $p < 0.05$ probability level (2-tailed), respectively.

$^{**}$ Correlation is significant at the $p < 0.01$ probability level (2-tailed), respectively.

## 4. Discussion

It is well known that the success of vegetation establishment in the degraded dryland largely depends on an extensive understanding of the relationships between soil characteristics and plant rooting features (Costantini et al., 2015; Neris et al., 2012; Huang et al., 2016; Wu et al., 2016c). Roots enmesh and realign soil particles and release exudates resulting in physical, chemical and biological alterations in the soil, which in turn influence the soil infiltration capacity (Bronick and Lal, 2005). Roots lead to the formation of well-connected macropores or channels, which normally grow into rigid pores broader than their own diameters (Logsdon and Allmaras, 1991). Plant roots are a major contributor to matrix flow mechanics as they create spatial voids that can be used as matrix flow pathways (Gish et al., 1998). In our study, the influence of matrix flow, as driven by root channels, on the process of soil infiltration was researched. The AIRS I and IIR of artificial grasslands correlated positively with the ARCD and the RCA in all grassland types (Table 4). The macropore flow is initiated at the soil surface or at a saturated or partially saturated soil layer, and the major flow process controlling macropore flow is the root channels flow (Weiler and Naef, 2003). Our results showed greater root diameter results in the higher IIRs (e.g., Hs). Channels created by plant roots may contribute to water transport, especially matrix flow (Bogner et al., 2010; Germann et al., 2012). In addition, the stem–root flow can help to create favorable conditions for plant growth under arid conditions (Li et al., 2009).

The infiltration capacity was strongly affected by the presence of certain plant functional groups (Wu et al., 2014), such as grasses and legumes. Grasses (e.g., *A. mongolicum* and *B. inermis*) have extensive fibrous root systems (Maiti, 2013) which were different from the root features of legumes (e.g., *M. sativa* and *A. adsurgens*) and shrubs (e.g., *H. scoparium* and *H. mongolicum*). The diameters of root channels in the leguminous grasslands and in the shrub grasslands were greater than those in the gramineous grasslands. Our results showed that the ARCD and RCA correlated positively with the AIRS I and IIR in the leguminous grasslands and in the gramineous grasslands (Table 4). The ARCD showed a positive correlation with AIRS II in the leguminous grasslands. These results were attributed to the unique root systems found in the leguminous grasslands and gramineous grasslands. The soil thickness is approximately 50 cm, and the plant roots are mainly distributed in the 0–30 cm soil layer in our study area (Wu et al., 2016c). Thus, no correlations were found among the ARCD, RCA, AIRS III and SIR (Table 4). Archer et al. (2002) reported that legumes increased and grasses decreased hydraulic conductivity, which is consistent with our results. It has been shown that the roots of legumes form stable macropores that act to increase soil infiltration more than grasses due to their higher root proliferation and root weight (Fischer et al., 2014; Wu et al., 2016c). The ARCD in the gramineous grasslands was approximately 1 mm, whereas in the leguminous grasslands and in the shrub grasslands it was more than 2 mm. For grass species, the growth of fibrous roots and an abundance of rhizomatous roots tend to reduce the infiltration rate by clogging the soil pore space and blocking water flow (Archer et al., 2002).

In addition, the diameter of root channels was significantly positively related to the AGB, the crown diameter, taproot diameter, lateral root diameter, and lateral root number; the root dry weight was significantly and positively related to the dry weight of the AGB (Wang et al., 2011). The AGB in the shrub grasslands and in the leguminous grasslands was higher than that in the gramineous grasslands. The results showed that the soil infiltration rates at different stages in the leguminous grasslands were higher than those in the gramineous grasslands. Li et al. (2013) reported that IIR increased with an increase in the root surface area density and was evidently correlated with root diameter. With an increase in the RCA, AIRS I and IIR sharply improved. Moreover, matrix flow pathways formed by root activity may have a positive impact on ground water quality. Water flow through void root channels could facilitate the biological degradation of preferentially moving agricultural chemicals (Gish et al., 1998).

## 5. Conclusions

The significant effect of root channels diameter and the area of root channels on soil water infiltration rates were investigated in different artificial grasslands. In general, the ARCD and RCA in leguminous grasslands and shrub grassland were greater than those in the gramineous grassland. Importantly, the ARCD and RCA were significantly and positively related to the average infiltration rate in AIRS I and the IIR. As the diameter of root channels increased, the IIR and AIRS I increased at rates of 31.13 and 14.60 mm $h^{-1}$ - $mm^{-1}$, respectively. Our results showed that plant root channels played a significant role in the soil infiltration capacity with the higher infiltration rates in leguminous grasslands and mixed sown grasslands than in gramineous grasslands. We suggest that leguminous grasslands or a combination of leguminous and gramineous species in grassland, should be closely considered for use in reclamation of mine soil in arid areas. Our research assists in understanding the influence of different types of vegetative on soil hydrological processes, and thus improves the understanding of the hydrology of reclaimed mine soils in arid areas.

## Acknowledgements

This research was funded by the Projects of Natural Science Foundation of China (NSFC 41525003, 41390463, 41371282), the Light of West China Program (XAB2015A04) and the Youth Innovation Promotion Association (2011288) of Chinese Academy of Sciences.

## References

Archer, N.A.L., Quinton, J.N., Hess, T.M., 2002. Below-ground relationships of soil texture, roots and hydraulic conductivity in two-phase mosaic vegetation in South-east Spain. J. Arid Environ. 52, 535–553.

Atanacković, N., Dragišić, V., Stojković, J., Papić, P., Zivanović, V., 2013. Hydrochemical characteristics of mine waters from abandoned mining sites in Serbia and their impact on surface water quality. Environ. Sci. Pollut. Res. Int. 20, 7615–7626.

Beven, K., Germann, P., 2013. Macropores and water flow in soils revisited. Water Resour. Res. 49, 3071–3092.

Bogner, C., Gaul, D., Kolb, A., Schmiedinger, I., Huwe, B., 2010. Investigating flow mechanisms in a forest soil by mixed-effects modelling. Eur. J. Soil Sci. 61 (6), 1079–1090.

Bronick, C.J., Lal, R., 2005. Soil structure and management: a review. Geoderma 124, 3–22.

Cerdà, A., 1997. Seasonal changes of the infiltration rates in a Mediterranean scrubland on limestone. J. Hydrol. 198, 209–225.

Clark, E.V., Zipper, C.E., 2016. Vegetation influences near-surface hydrological characteristics on a surface coal mine in eastern USA. Catena 139, 241–249.

Costantini, E.A.C., Branquinho, C., Nunes, A., Schwilch, G., Stavi, I., Valdecantos, A., Zucca, C., 2015. Soil indicators to assess the effectiveness of restoration strategies in dryland ecosystems. Solid Earth 7, 397–414.

Devitt, D.A., Smith, S.D., 2002. Root channel macropores enhance downward movement of water in a Mojave desert ecosystem. J. Arid Environ. 50 (1), 99–108.

Fischer, C., Roscher, C., Jensen, B., Eisenhauer, N., Baase, J., Attinger, S., Scheu, S., Weisser, W.W., Schumacher, J., Hildebrandt, A., 2014. How do earthworms, soil texture and plant composition affect infiltration along an experimental plant diversity gradient in grassland? PLoS ONE 9 (2), e98987.

Germann, P.F., Lange, B., Lüscher, P., 2012. Preferential flow dynamics and plant rooting systems. In: Hydropedology, pp. 121–141.

Gish, T.J., Gimenez, D., Rawls, W.J., 1998. Impact of roots on ground water quality. Plant Soil 200 (1), 47–54.

Huang, Z., Tian, F.P., Wu, G.L., Liu, Y., Dang, Z.Q., 2016. Legume grasslands are in favour of promoting precipitation infiltration than gramineous grasslands in the arid regions. Land Degrad. Develop. http://dx.doi.org/10.1002/ldr.2635.

Khan, S., Hanjra, M.A., Mu, J.X., 2009. Water management and crop production for food security in China: a review. Agric. Water Manage. 96, 349–360.
Lei, T.W., Chuo, R.Y., Zhao, J., Shi, X.N., Liu, L., 2010. An improved method for shallow water flow velocity measurement with practical electrolyte input. J. Hydrol. 390, 45–56.
Lei, T.W., Mao, L.L., Li, X., Liu, H., Huang, X.F., Zhang, Y.N., 2007. Method for measuring soil infiltrability with linear run-on of water. Trans. Chin. Soc. Agric. Eng. 23 (1), 1–5.
Lei, T.W., Yan, Y., Shi, X.N., Chuo, R.Y., Zhao, J., 2013. Measuring velocity of water flow within gravel layer with electrolyte tracer method under pulse boundary model. J. Hydrol. 500, 37–44.
Li, J.X., He, B.H., Chen, Y., 2013. Root features of typical herb plants for hillslope protection and their effects on soil infiltration. Acta Ecol. Sinica 33 (5), 1535–1547.
Li, X.Y., Yang, Z.P., Li, Y.T., Lin, H., 2009. Connecting ecohydrology and hydropedology in desert shrubs: stemflow as a source of preferential flow in soils. Hydrol. Earth Syst. Sci. Discuss. 13 (7), 1133–1144.
Logsdon, S.D., Allmaras, R.R., 1991. Maize and soybean root clustering as indicated by root mapping. Plant Soil 131 (2), 169–176.
Maiti, S.K., 2013. Ecorestoration of the Coalmine Degraded Lands. Springer, New York.
Mao, L.L., Lei, T.W., Bralts, V.F., 2011. An analytical approximation method for the linear source soil infiltrability measurement and its application. J. Hydrol. 411, 169–177.
Mao, L.L., Li, Y.Z., Hao, W.P., Mei, X.R., Bralts, V.F., Li, H.R., Guo, R., Lei, T.W., 2016. An approximate point source method for soil infiltration process measurement. Geoderma 264, 10–16.
Michaelides, K., Lister, D., Wainwright, J., Parsons, A.J., 2009. Vegetation controls on small-scale runoff and erosion dynamics in a degrading dryland environment. Hydrol. Process. 23, 1617–1630.
Moreno-de Las Heras, M., Merino-Martín, L., Nicolau, J.M., 2009. Effect of vegetation cover on the hydrology of reclaimed mining soils under Mediterranean-continental climate. Catena 77, 39–47.
Neris, J., Jiménez, C., Fuentes, J., Morillas, G., Tejedor, M., 2012. Vegetation and land-use effects on soil properties and water infiltration of Andisols in Tenerife (Canary Islands, Spain). Catena 98, 55–62.
Pinheiro, J., Bates, D., DebRoy, S., R Core Team, 2016. nlme: Linear and Nonlinear Mixed Effects Models. R package version 3.1-128, <https://CRAN.R-project.org/package=nlme>.
Rechel, E.R., Carter, L.M., 1992. Infiltration rate of a sandy loam soil: effects of traffic, tillage, and plant roots. Soil Sci. Soc. Am. J. 56 (3), 908–913.
Shi, H., Shao, M.A., 1999. Soil and water loss from the Loess Plateau in China. J. Arid Environ. 45, 9–20.
Shi, Z.H., Fang, N.F., Wu, F.Z., Wang, L., Yue, B.J., Wu, G.L., 2012. Soil erosion processes and sediment sorting associated with transport mechanisms on steep slopes. J. Hydrol. 454–455, 123–130.
Van Schaik, N.L.M.B., 2009. Spatial variability of infiltration patterns related to site characteristics in a semi-arid watershed. Catena 78, 36–47.
Wang, F.G., Yu, L.Q., Tian, Z.H., Su, D., Sun, J.J., 2011. Root characteristics and the relationship with yield of 18 alfalfa cultivars. Chin. J. Grassland 33 (4), 51–57.
Wang, Y.Q., Shao, M.A., 2013. Spatial variability of soil physical properties in a region of the loess plateau of PR China subject to wind and water erosion. Land Degrad. Dev. 24 (3), 296–304.
Weiler, M., Naef, F., 2003. An experimental tracer study of the role of macropores in infiltration in grassland soils. Hydrol. Process. 17 (2), 477–493.
Wu, G.L., Zhang, Z.N., Wang, D., Shi, Z.H., Zhu, Y.J., 2014. Interactions of soil water content heterogeneity and species diversity patterns in semi-arid steppes on the Loess Plateau of China. J. Hydrol. 519, 1362–1367.
Wu, G.L., Liu, Y., Fang, N.F., Deng, L., Shi, Z.H., 2016a. Soil physical properties response to grassland conversion from cropland on the semi-arid area. Ecohydrol. 9, 1471–1479.
Wu, G.L., Liu, Y., Tian, F.P., Shi, Z.H., 2016b. Legumes functional group promotes soil organic carbon and nitrogen storage by increasing plant diversity. Land Degrad. Dev. http://dx.doi.org/10.1002/ldr.2570.
Wu, G.L., Yang, Z., Cui, Z., Liu, Y., Fang, N.F., Shi, Z.H., 2016c. Mixed artificial grasslands with more roots improved mine soil infiltration capacity. J. Hydrol. 535, 54–60.
Xin, P., Yu, X.Y., Lu, C.H., Li, L., 2016. Effects of macro-pores on water flow in coastal subsurface drainage systems. Adv. Water Resour. 87, 56–67.
Yang, H.J., Jiang, L., Li, L.H., Li, A., Wu, M.Y., Wan, S.Q., 2012. Diversity-dependent stability under mowing and nutrient addition: evidence from a 7-year grassland experiment. Ecol. Lett. 15, 619–626.
Younger, P.L., Wolkersdorfer, C., 2004. Mining impacts on the fresh water environment: technical and managerial guidelines for catchment scale management. Mine Water Environ. 23, 2–80.
Zhu, W.Z., Cheng, S., Cai, X.H., He, F., Wang, J.X., 2009. Changes in plant species diversity along a chronosequence of vegetation restoration in the humid evergreen broad-leaved forest in the Rainy Zone of West China. Ecol. Res. 24, 315–325.